Renal Cell Carcinoma: A Comprehensive in Silico Study in Searching for Therapeutic Targets

Mohammadjavad Naghdibadi
Isfahan University of Medical Sciences
Maryam Moemeni
The University of Isfahan
Parvin Yavari
Isfahan University of Medical Sciences
Alieh gholaminejad
Isfahan University of Medical Sciences
Amir Roointan (roointan@res.mui.ac.ir)
Isfahan University of Medical Sciences

Research Article

Keywords: clear cell renal cell carcinoma, Transcriptomics, Systems biology, Weighted gene co-expression network, Drug target

Posted Date: June 29th, 2022

DOI: https://doi.org/10.21203/rs.3.rs-1782898/v1

Abstract

Background: Renal cell carcinoma (RCC) is recognized as one of the main causes of illness and death worldwide. Understanding the molecular mechanisms in RCC pathogenesis is of utmost importance for discovering novel therapeutic targets and developing efficient drugs. With the application of a comprehensive in silico analysis of the RCC-related array sets, the main objective of this study was to discover the top molecules and pathways in the pathogenesis of this cancer.

Methods: RCC microarray datasets were downloaded from the Gene Expression Omnibus database and after quality checking, normalization, and analysis using the limma algorithm, differentially expressed genes (DEGs) were identified considering the adjusted p-value < 0.049. The intensity values of the identified DEGs were introduced to the WGCNA algorithm for the construction of co-expression modules. Functional enrichment analyses were performed using the DEGs in the disease correlated module and hub genes were identified among the top genes in a protein-protein interaction network and the disease most correlated module. The expression analysis of hub genes was done by utilizing GEPIA and GSCA server was used to make a comparison between the expression patterns of hub genes in ccRCC and other cancers. DGIdb database was utilized to identify the hub genes related drugs.

Results: Three datasets including GSE11151, GSE12606, and GSE36897 were retrieved, merged, normalized, and analyzed. Using WGCNA the DEGs were clustered into eight different modules. Translocation of ZAP-70 to immunological synapse, endosomal/vacuolar pathway, cell-surface interactions at the vascular wall, and immune-related pathways were the topmost enriched terms for the ccRCC correlated DEGs. Twelve genes including PTPRC, ITGAM, TLR2, CD86, PLEK, TYROBP, ITGB2, RAC2, CSF1R, CCR5, CCL5, and LCP2 were introduced as hub genes. All the 12 hub genes were up-regulated in ccRCC samples and showed a positive correlation with the infiltration of different immune cells. According to the DGIdb database, 127 drugs including tyrosine kinase inhibitors, glucocorticoids, and chemotaxis targeting molecules were identified to interact with the hub genes.

Conclusions: By utilizing an integrative bioinformatics approach, this experiment shed a light on the underlying signaling pathways in the pathogenesis of ccRCC and introduced several potential therapeutic targets for repurposing or developing novel drugs for an efficient treatment of this cancer.

Background

Renal cell carcinoma (RCC) is one of the leading causes of death and morbidity in the world. With 431288 new cases and 179368 deaths in 2020, this cancer is considered an urgent global problem [1]. So altogether, RCC is an evolving health issue that requires more effective preventive/therapeutic actions. About 70%-75% of RCC types are clear cell RCC (ccRCC) that are recognized by their clear appearance in pathology [2]. ccRCC cases are usually resistant to radiotherapy and chemotherapy; therefore, surgery is still the preferred treatment option for the patients [3]. However, this approach is only effective in the early stages of cancer (when it is localized). In metastatic forms (systemic spreading of ccRCC), targeted

therapies such as tyrosine kinase inhibitors (TKIs), VEGF inhibitors, or mTOR inhibitors are usually prescribed. In addition, immune checkpoint inhibitors were among the recently included therapeutics in the FDA-approved ccRCC treatment list [4]. Although such treatments can improve survival rates in patients, drug responses are not satisfactory, and eventually, drug resistance develops in most patients [5]. Therefore, more investigations are required to not only have a deeper understanding of ccRCC pathogenesis but also to discover novel druggable key elements in its pathogenesis.

Although various genetic events like 3p chromosome arm loss, VHL gene mutation, STED2 mutation, and KDM5C mutation have shown to be linked with the pathogenesis of ccRCC, the exact underlying molecular mechanisms of this cancer are not yet fully understood [3]. In this context, systems biology approaches could be beneficial in dealing with high-throughput data coming from cancer patients and exploring the complexity behind such convoluted pathological phenomena [6].

Recently, a rising number of researchers have examined high-throughput datasets to catch a better understanding of the biological roots of various diseases [7, 8]. In this context, analyzing and interpreting transcriptomics datasets with different bioinformatics approaches could provide a holistic view of expressional changes in cancer versus normal states [9].

In this context, the Weighted Gene Co-Expression Network Analysis (WGCNA) algorithm is one of the well-known clustering tools for identifying co-expressed and disease correlated genes in expression datasets [10–12]. So far, a large number of studies have used the WGCNA to investigate various biological processes in different conditions like genetic disorders, cancers, and other chronic diseases like nephropathy and Alzheimer's aiming for discovering new biomarkers or therapeutic targets [13, 14].

This study aimed to reveal the cancer-related underlying molecular mechanisms and introduce the principal hub genes in ccRCC pathogenesis by analyzing available ccRCC microarray datasets using network analysis and the WGCNA algorithm. After analyzing the ccRCC-related datasets, the intensity values of the discovered differentially expressed genes (DEGs) were passed to WGCNA in the R environment. Then, by identifying the disease correlated module, the classified DEGs in the selected module were subjected to functional enrichment analyses, and the hub genes were spotted by considering the top genes in the protein-protein interaction (PPI) network, including all the DEGs and a list ordered by module membership (kME) values of genes in the selected module. The hub genes also were considered for further examinations like expressional validations and drug repositioning. The workflow of the present study is shown in Fig. 1.

Materials And Methods

Dataset qualification and analysis

Gene Expression Omnibus (https://www.ncbi.nlm.nih.gov/geo/) was used to search and download the RCC microarray datasets. Previous to the primary analysis step, principal component analysis (PCA) was accomplished to distinguish and eliminate probable outliers. Normalization, removal of multiple genes-

related probes, and analysis were performed with the help of the Networkanalyst online tool (http://www.networkanalyst.ca). Linear Model for Microarray Analysis (Limma) was selected for the analysis procedure, and a false discovery rate (FDR) cutoff <0.049 was considered to identify the significant DEGs [15, 16].

WGCNA: Construction of gene co-expression networks

WGCNA algorithm was applied in order to identify the co-expression modules among the intensity values of the identified DEGs. A matrix containing the intensity files of the identified DEGs was introduced to the WGCNA, and next to the sample clustering, the best soft-threshold power was selected using the 'pickSoftThreshold' function in the package. The best soft-threshold power (value = 7) was selected based on the mean connectivity and degree of independence values. Afterward, several steps, including adjacency matrix construction, module identification (minModuleSize = 30), topological overlap matrix (TOM) calculation, construction of modules, and finally, dynamic branch cutting (merging threshold: 0.25), were conducted independently to reach the co-expression modules. Moreover, after assessing the correlation between two states (cancer vs. normal) and the co-expression modules, the most correlated module was identified [10].

Functional enrichment analysis

Functional enrichment analyses, including gene ontology (GO) and pathway enrichment, were performed for the extracted DEGs from the module of interest. These analyses (significant enrichment threshold: P<0.05) were performed using Cytoscape software (version 3.9.1) and the CluGO module (version 2.5.7) [17, 18].

Hub gene identification

Candidate hub gene identification was performed by considering both module membership (kME) and DEG network centrality (degree) values in a constructed PPI network. In detail, after PPI network construction using all DEGs, the top 100 genes with a high degree of connectivity were listed. On the other hand, the DEGs with kME values of more than 0.8 in the module were extracted and recorded. Lastly, hub genes were selected as the common ones in both lists. Contraction of the PPI network was performed using the STRING database (confidence>0.4), and Cytoscape (v.3.9.1) was utilized for network visualizations and analysis [18, 19].

Verification of hub genes and stage analysis

Gene Expression Profiling Interactive Analysis (GEPIA, http://gepia.cancer-pku.cn/) was applied for the expression analysis of hub genes [20]. The expression levels of the hub genes in 100 normal kidney tissues and 523 ccRCC tissues were plotted to compare the expression levels between the two states. The log2 transformed TPM (Transcripts Per Kilobase Million) of RNAseq data was used for plotting the box plots. The correlation of expressions of hub genes with cancer pathological stages was examined by

GEPIA. The log2 transformed TPM values were used for plotting stage plots. The considered threshold for this analysis was Pr (>F) < 0.05.

Expression patterns of the hub genes in other cancers

Gene Set Cancer Analysis (GSCA) server was utilized to assess the expression patterns and values of the hub genes in ccRCC and other cancers [21]. The GSCA is performing differential expression analysis of paired normal and tumor tissues from TCGA based on normalized RSEM (RNA-Seq by Expectation-Maximization) mRNA expression. The data from 11-114 paired tumor and normal samples were utilized in the analysis for each cancer type. T-test was used to estimate the p-value, and FDR was used as the correction method.

Drug-gene interaction identification:

To identify potential drugs for the treatment of ccRCC, we performed a drug-gene interaction assessment using DGIdb (Drug–Gene Interaction Database, https://www.dgidb.org/). DGIdb is an open-source project that freely provides gene-drug interactions from 22 trusted sources [22]. The tool was applied to obtain hub genes-drug interactions. Then, a network of the potential drugs and targeted hub genes was constructed by Cytoscape (version 3.9.1) [18].

Immune cell infiltration prediction

Spearman correlation between hub genes GSVA scores and different immune cells was exported as a heatmap using the GSCA server based on the ImmuCellAI method and the Cancer Genome Atlas ccRCC transcriptomics information (FDR ≤ 0.05) [21, 23].

Results

identified based on the FDR cutoff.

All the steps of the present work are shown in figure 1. Three RCC datasets, including GSE11151, GSE12606, and GSE36897, were selected and retrieved from the GEO database. Due to the same platform, all three datasets were merged to have a meta dataset, including 58 and 32 cancer and control samples, respectively. PCA as a valuable tool to check the quality of datasets was performed before the analysis [15] (Figure 2A). Likewise, the quantile normalization was performed to assure the similarity of the expression distributions of each sample across the entire meta dataset. After analysis, 7411 significant DEGs, including 4179 down-regulated and 3232 up-regulated genes, were detected (FDR cutoff <0.049) and subjected to further analysis. The volcano plot of the analyzed dataset and a heatmap for the top 50 DEGs based on FDR are shown in figures 2B and C. The results of the DEG analysis are provided in sheet 1 of supplementary file 1.

Co-expression module construction: 8 different co-expressed modules were identified

Co-expression module identification was carried out using the WGCNA algorithm in the R software environment. Using this package, we performed sample clustering, constructed co-expression networks, and finally recognized the highly correlated module to the RCC state [10]. Sample clustering was performed, and each sample was dedicated to either disease or control state (Figure 3A). The resulting scale independence and mean connectivity platforms are shown in figure 3 B. According to the resulting platforms, a best soft-threshold (soft-threshold: 7) was designated to get an approximate scale-free topology. Further on, after performing hierarchical clustering and module merging, the DEGs were classified into eight different co-expression modules, including blue, black, brown, pink, purple, magenta, red, and salmon (Figures 4A, B, and D). The number and names of the classified DEGs in each module are listed in sheet 2 of supplementary file 1. The constructed heatmap plot (Figure 4 C) revealed the accuracy of the module division and the topological overlap adjacency among genes in modules.

Module-trait correlation analysis: pink module was identified as the ccRCC highly correlated module

The correlations between modules and phenotypes (cancer and normal) were checked and the pink module with 2441 DEGs was recognized as the most disease relevant module (r = 0.84; P = 2E-25). (Figure 4 E). Other modules with a positive correlation to the disease state were including magenta (r = 0.53; P = 7E-8), black (r = 0.58; P = 2E-9), purple (r = 0.56; P = 8E-9) and red (r = 0.62; P=9E-11). Other modules including salmon (r = -0.57; P = 5E-9), blue (r = -0.91; P = 3E-35) and brown (r = -0.72; P = 2E-15) had negative correlations with the cancer state. Scatter plot of the gene significance (GS) vs kME values of all DEGs in the pink module is shown in figure 4 F. The high correlation between the values of GS and kME in the pink module (r = 0.9, p<1e-200), proposing the association of genes with both the module eigengene and the disease state.

Functional enrichment analysis: Genes of the pink module were mainly related to the pathways involved in the immune system

The results of functional enrichment analyses of the DEGs in the pink module are shown in Table 1 (top 10 terms). Based on the results of Reactome pathway analysis, the DEGs were mostly enriched in “translocation of ZAP-70 to immunological synapse”, “endosomal/vacuolar pathway”, “cell surface interactions at the vascular wall”, and “immune-related pathways”. The enriched terms in the biological process section also confirmed the results of Reactome pathway enrichment, where the primarily enriched terms were related to immunological processes like “regulation of neutrophil activation”, “interleukins, and interferon-mediated signaling pathways”, and “Fc receptor-mediated inhibitory signaling pathway”. In terms of molecular function, the top enriched terms were “transporter associated with antigen processing (TAP) binding”, “T cell receptor binding”, “MHC, and cytokine receptors activities”. In addition, the top cellular component terms were “complement component C1 complex”, “MHC protein complex”, “NLRP3 inflammasome complex”, “integral component of lumenal side of endoplasmic reticulum membrane” and “phagocytic cup”.

PPI network construction and hub gene identification: 12 hub genes were identified among top genes in both PPI network and WGCNA analyses

A PPI network with 6802 nodes and 146523 edges was constructed, including almost all the classified DEGs in the eight modules. The network is uploaded to the NEDx server and is accessible through the link:

https://www.ndexbio.org/#/network/50894774-9c60-11ec-b3be-0ac135e8bacf?accesskey=5fda0e58489fd8a029aad792b07c7200d027a70439915453c3a0d1d6a7d7d431.

The constructed network was analyzed, and the top 100 DEGs based on the degree of centrality were identified. On the other hand, the top DEGs based on kME and GS values (171 DEGs) were identified and listed among the DEGs in the pink module (Table 2). Common DEGs of two lists were 12 genes named as hubs in this study. The hubs included “protein tyrosine phosphatase receptor type C (PTPRC)”, “integrin subunit alpha M (ITGAM)”, “Toll-like receptor 2 (TLR2)”, “CD86 molecule (CD86)”, “pleckstrin (PLEK)”, “TYRO protein tyrosine kinase binding protein (TYROBP)”, “integrin subunit beta 2 (ITGB2)”, “Rac family small GTPase 2 (RAC2)”, “colony-stimulating factor 1 receptor (CSF1R)”, “C-C motif chemokine receptor 5 (CCR5)”, “C-C motif chemokine ligand 5 (CCL5)”, “lymphocyte cytosolic protein 2 (LCP2)”.

Hub genes expressional validation and stage analysis: the 12 hub genes showed upregulation patterns

Based on the expression analysis results of 100 normal kidneys and 523 ccRCC samples by GEPIA, all the 12 hub genes showed upregulation patterns in ccRCC samples compared to normal samples (Figure 5 A). Moreover, in the stage analysis step by GEPIA, four out of twelve hub genes, including CCR5, RAC2, TYROBP, and CCL5, showed significant changes during different ccRCC stages (Figure 5 B). These findings confirmed the expressional state of the hub DEGs in the present study.

Hub gene expression levels in ccRCC vs. other cancers: The expressional pattern of 12 hub genes were specific to ccRCC

GSCA is an integrated database for gene set analysis in cancers. Using this database, we compared the differential expression values of hub genes with other cancers and the results showed an exclusive alteration pattern in the expressional values of the hub genes in ccRCC samples (Figure 6 A).

Immune cells infiltration prediction: Hub genes showed a positive correlation with the infiltration of different immune cells

In this step, the GSCA database was utilized to obtain the type and patterns of immune cell infiltration in ccRCC. The result of this step is shown in figure 6 B. Based on findings, there was a positive correlation between the expression of the 12 hub genes and “T helper 1 cells”, “macrophage cells”, “induced Regulatory T cells (iTreg)”, “exhausted T cells”, “type 1 regulatory cells”, “CD8-positive T cells”, “central memory T cells”, “T follicular helper cells (Tfh)”, natural Treg, dendritic cells (DC), cytotoxic cells, and “CD4 positive T cells”. On the other hand, a negative correlation was observed between the expression of hub genes and “neutrophil cells”, “T helper 17”, “CD8_naive cells”, “T helper 2 cells”, “CD4_naive cells”, “effector memory cells”, and “monocyte immune cells”. In addition, the hub genes had a positive correlation with the general immune cell infiltration score.

Drug-gene interaction analysis: Various drugs were identified to interact with the hub genes

To identify the hubs' most related drugs, the DGIdb database was searched using the 12 hub DEGs. In this step, 60, 15, 18, 10, 12, 4, 6, and 2 drugs were found for CSF1R, CCR5, ITGB2, ITGAM, PTPRC, TLR2, CD86, and RAC2, respectively. A network comprising the hub genes and their related drug molecules is shown in figure 7.

Discussion

In this integrative in silico study, 12 hub genes were identified as key genes in the pathogenesis of ccRCC. Notably, some of the identified hub genes in the present study were previously recognized as key players in the pathogenesis of ccRCC [24–28]. A brief description of the identified hub genes is provided in supplementary file 2. In the present study, the selection of hubs was based on two different approaches considering the relationships between genes in a PPI network and expressional correlations among them in co-expression networks. The identified hub genes had high interaction degrees in the PPI network, as well as high module membership values in the disease most correlated co-expressed module. All the 12 hub genes were among the up-regulated genes in ccRCC vs. normal conditions. The expressional validation results using the TCGA database also were in line with our analysis. Moreover, the expressional pattern of the hub genes was different in other cancers which might indicate the exclusive role of these 12 genes in ccRCC pathogenesis (Fig. 6A). In addition, based on the stage analysis results, four of the hub genes showed increasing patterns in their expression in different stages of ccRCC. Accordingly, these four genes including TYROBP, CCL5, CCR5, and RAC2 might have a part in the progression of ccRCC, and as a biomarker, the expression levels of these genes can indicate the stages of the disease.

Based on gene ontology results, immunological pathways were the most enriched terms for the DEGs in the disease most correlated module. Also, all of the identified hub genes were involved in immune response processes. Such findings are in line with previous histopathologic and transcriptomic studies in which ccRCC is recognized as one of the most immune cell infiltrated neoplasms [29, 30]. Based on our results, the expression of the identified hub genes is associated with increased Treg and decreased Th17 and CD8 + T immune cells infiltration in the tumor microenvironment; According to some experiments, infiltration of these cells predicts poor prognosis for ccRCC patients [31]. Accordingly, it is suggested that the identified hub genes are involved in the ccRCC immune microenvironment dynamics. Specifically, T cell immune checkpoint inhibitors have created a new promising era in the treatment of ccRCC, and current checkpoint inhibitors (alone or in combination with tyrosine kinase inhibitors) are becoming the standard of treatment for metastatic ccRCC [30]. In addition, our gene ontology analysis showed that the innate immune responses (like IFN pathways, regulation of neutrophil activation and degranulation, antigen processing and presentation, Toll-like Receptor Cascades, and Fc receptor signaling) have a principal value in the ccRCC pathogenesis. Such findings are consistent with other studies indicating the importance of innate immune cells in ccRCC immunology such as myeloid-derived suppressor cells (MDSCs) [29, 32]. Therefore, the outlook of ccRCC immunotherapy might need to pass through from only focusing on the adaptive immune system.

In the next step of this work, we focused on drug-gene interaction identification, to propose candidates for more evaluations in drug repurposing studies. Based on the results, 127 drugs were identified to interact with the eight hub genes. The results of this part indicated the importance and therapeutic potential of the identified hub genes in ccRCC. Interestingly, some of the identified drugs (Sunitinib, Pazopanib, sorafenib) that target CSF1R are currently applied for ccRCC treatment as TKIs [4]; Notably, CSF1R inhibition has recently gained more attention for targeting immune suppression in solid tumors [33]. Furthermore, ipilimumab (anti-CTLA-4) which is responsible for suppressing the interaction of CD28 and CD86, is another approved drug for ccRCC immunotherapy [30].

Among the predicted drugs, there were also some immunosuppressive ones like hydrocortisone, prednisone, dexamethasone, methylprednisolone (glucocorticoids), Adalimumab, Infliximab, Etanercept (anti-TNF alpha antibodies), and Indomethacin (NSAIDs) that target CD86, ITGB2, ITGAM, PTPRC, and CD86. Interestingly, there are some clinical case reports of spontaneous remission following glucocorticoid therapy in ccRCC patients [34–37]. Despite such reports, we believe glucocorticoids could be potential drug candidates for the treatment of ccRCC [38]. Likewise, different *in vitro* and *in vivo* studies have shown the inhibitory effects of these drugs on ccRCC [39, 40]. Although immunosuppressive, like several approved TKIs for the treatment of ccRCC, glucocorticoids have anti-angiogenesis functions [41, 42]. In addition, even though some of the TKIs have immunomodulatory properties [43], different studies have shown their ability in reprogramming the tumor immune microenvironment and promotion of anti-tumor immunity [32]. Also, there are some pieces of evidence indicating the anti-proliferative/immunostimulatory effect of anti-TNF alpha antibodies and Indomethacin in ccRCC cases [44–47].

Other identified drugs were chemotaxis targeting molecules including Rovelizumab, which is known as a safe and tolerable anti-CD18/CD11b (ITGB2/ITGAM), and Maraviroc that target the CCR5/CCL5 axis [48, 49]. It was shown that the CD18/CD11b complex on macrophages and neutrophils has a role in the recruitment of myeloid-derived suppressor cells (MDSCs) to the tumor microenvironment. Currently, the efficiency of several CD18/CD11b inhibitors for solid tumors therapy is under evaluation [48]. Likewise, the role of the CCR5/CCL5 axis in immunosuppressive cell recruitment in tumor progression was shown by previous studies. Maraviroc, as an inhibitor of this axis, is approved for the treatment of HIV-1 infection [49–51]. Resveratrol hexanoic acid, a resveratrol derivate with improved pharmacokinetic functions, was another identified drug for the hub genes in ccRCC condition (targeting TLR2) [52]. Several studies have indicated the immunostimulatory and tumor-suppressing effect of this FDA-approved antioxidant agent in ccRCC. Therefore, considering the excellent safety profile of Resveratrol, it can be a good target for further investigations in the treatment of the ccRCC [53–56].

Conclusion

By utilizing an integrative bioinformatics approach, this in silico study tried to shed light on the underlying mechanisms in the pathogenesis of ccRCC. Moreover, twelve genes were introduced as potential therapeutic targets to hinder the progression of ccRCC. The introduced hubs could also be the target of

future investigations in order to explore their exact roles in the progression of this cancer. Recently, single-cell RNA sequencing has been recognized as an excellent solution for unraveling the complex aspect of the tumor microenvironment. Therefore, our next step is to identify the gene expression profiles of these 12 genes in different ccRCC tumor microenvironment cell populations, especially immune cells.

Declarations

Acknowledgments

We thank Regenerative Medicine Research Center members for their help in some parts of the bioinformatic analysis steps.

Authors' contributions

Amir Roointan participated in the study design, analysis of the dataset using the WGCNA algorithm, and interpretation of data. Mohammadjavad Naghdibadi participated in data analysis and drafting of the main text. Maryam Moemeni and Parvin Yavari wrote some parts of the manuscript and prepared the figures. Alieh Gholaminejad participated in dataset selection and data analysis. All authors reviewed the manuscript.

Funding

This work was supported by the Isfahan University of Medical Sciences [grant number 2400109].

Availability of data and materials

The analyzed datasets by the present study is available in the GEO repository:

[https://www.ncbi.nlm.nih.gov/geo/query/acc.cgi?acc=GSE11151]

[https://www.ncbi.nlm.nih.gov/geo/query/acc.cgi?acc=GSE12606]

[https://www.ncbi.nlm.nih.gov/geo/query/acc.cgi?acc=GSE36897]

Declarations

Ethics approval and consent to participate

Not applicable.

Consent for publication

Not applicable.

Competing interests

The authors declare that they have no competing interests.

References

1. Sung H, Ferlay J, Siegel RL, Laversanne M, Soerjomataram I, Jemal A, et al. Global Cancer Statistics 2020: GLOBOCAN Estimates of Incidence and Mortality Worldwide for 36 Cancers in 185 Countries. CA: A Cancer Journal for Clinicians. 2021;71:209–49.
2. Barata PC, Rini BI. Treatment of renal cell carcinoma: Current status and future directions. CA: A Cancer Journal for Clinicians. 2017;67:507–24.
3. Hsieh JJ, Purdue MP, Signoretti S, Swanton C, Albiges L, Schmidinger M, et al. Renal cell carcinoma. Nature Reviews Disease Primers. 2017;3:17009.
4. Choueiri TK, Motzer RJ. Systemic Therapy for Metastatic Renal-Cell Carcinoma. The New England journal of medicine. 2017;376:354–66.
5. Chen W, Pan X, Cui X. RCC Immune Microenvironment Subsequent to Targeted Therapy: A Friend or a Foe? Frontiers in oncology. 2020;10:573690.
6. Werner HMJ, Mills GB, Ram PT. Cancer Systems Biology: a peek into the future of patient care? Nature Reviews Clinical Oncology. 2014;11:167–76.
7. Soon WW, Hariharan M, Snyder MP. High-throughput sequencing for biology and medicine. Molecular systems biology. 2013;9:640.
8. Roointan A, Gheisari Y, Hudkins KL, Gholaminejad A. Non-invasive metabolic biomarkers for early diagnosis of diabetic nephropathy: Meta-analysis of profiling metabolomics studies. Nutrition, Metabolism and Cardiovascular Diseases. 2021;31:2253–72.
9. Cieślik M, Chinnaiyan AM. Cancer transcriptome profiling at the juncture of clinical translation. Nature Reviews Genetics. 2018;19:93–109.
10. Langfelder P, Horvath S. WGCNA: an R package for weighted correlation network analysis. BMC Bioinformatics. 2008;9:559.
11. Gholaminejad A, Roointan A, Gheisari Y. Transmembrane signaling molecules play a key role in the pathogenesis of IgA nephropathy: a weighted gene co-expression network analysis study. BMC immunology. 2021;22:73.
12. Gholaminejad A, Ghaeidamini M, Simal-Gandara J, Roointan A. An Integrative in silico Study to Discover Key Drivers in Pathogenicity of Focal and Segmental Glomerulosclerosis. Kidney and Blood Pressure Research. 2022. https://doi.org/10.1159/000524133.
13. Xia L-Y, Tang L, Huang H, Luo J. Identification of Potential Driver Genes and Pathways Based on Transcriptomics Data in Alzheimer's Disease. Frontiers in aging neuroscience. 2022;14:752858.
14. Gholaminejad A, Fathalipour M, Roointan A. Comprehensive analysis of diabetic nephropathy expression profile based on weighted gene co-expression network analysis algorithm. BMC Nephrology. 2021;22:245.

15. Yeung KY, Ruzzo WL. Principal component analysis for clustering gene expression data. Bioinformatics (Oxford, England). 2001;17:763–74.
16. Zhou G, Soufan O, Ewald J, Hancock REW, Basu N, Xia J. NetworkAnalyst 3.0: a visual analytics platform for comprehensive gene expression profiling and meta-analysis. Nucleic acids research. 2019;47:W234–41.
17. Bindea G, Mlecnik B, Hackl H, Charoentong P, Tosolini M, Kirilovsky A, et al. ClueGO: a Cytoscape plug-in to decipher functionally grouped gene ontology and pathway annotation networks. Bioinformatics (Oxford, England). 2009;25:1091–3.
18. Shannon P, Markiel A, Ozier O, Baliga NS, Wang JT, Ramage D, et al. Cytoscape: a software environment for integrated models of biomolecular interaction networks. Genome research. 2003;13:2498–504.
19. Szklarczyk D, Gable AL, Lyon D, Junge A, Wyder S, Huerta-Cepas J, et al. STRING v11: protein-protein association networks with increased coverage, supporting functional discovery in genome-wide experimental datasets. Nucleic acids research. 2019;47:D607–13.
20. Tang Z, Li C, Kang B, Gao G, Li C, Zhang Z. GEPIA: a web server for cancer and normal gene expression profiling and interactive analyses. Nucleic acids research. 2017;45:W98–102.
21. Liu C-J, Hu F-F, Xia M-X, Han L, Zhang Q, Guo A-Y. GSCALite: a web server for gene set cancer analysis. Bioinformatics (Oxford, England). 2018;34:3771–2.
22. Freshour SL, Kiwala S, Cotto KC, Coffman AC, McMichael JF, Song JJ, et al. Integration of the Drug–Gene Interaction Database (DGIdb 4.0) with open crowdsource efforts. Nucleic Acids Research. 2021;49:D1144–51.
23. Miao Y-R, Zhang Q, Lei Q, Luo M, Xie G-Y, Wang H, et al. ImmuCellAI: A Unique Method for Comprehensive T-Cell Subsets Abundance Prediction and its Application in Cancer Immunotherapy. Advanced science (Weinheim, Baden-Wurttemberg, Germany). 2020;7:1902880.
24. Qu G, Wang H, Yan H, Liu G, Wu M. Identification of CXCL10 as a Prognostic Biomarker for Clear Cell Renal Cell Carcinoma. Frontiers in oncology. 2022;12:857619.
25. Song E, Song W, Ren M, Xing L, Ni W, Li Y, et al. Identification of potential crucial genes associated with carcinogenesis of clear cell renal cell carcinoma. Journal of cellular biochemistry. 2018;119:5163–74.
26. Lin J, Yu M, Xu X, Wang Y, Xing H, An J, et al. Identification of biomarkers related to CD8+ T cell infiltration with gene co-expression network in clear cell renal cell carcinoma. Aging. 2020;12:3694–712.
27. Li F, Jin Y, Pei X, Guo P, Dong K, Wang H, et al. Bioinformatics analysis and verification of gene targets for renal clear cell carcinoma. Computational biology and chemistry. 2021;92:107453.
28. Wang A, Chen M, Wang H, Huang J, Bao Y, Gan X, et al. Cell Adhesion-Related Molecules Play a Key Role in Renal Cancer Progression by Multinetwork Analysis. BioMed research international. 2019;2019:2325765.

29. Díaz-Montero CM, Rini BI, Finke JH. The immunology of renal cell carcinoma. Nature reviews Nephrology. 2020;16:721–35.
30. Braun DA, Bakouny Z, Hirsch L, Flippot R, Van Allen EM, Wu CJ, et al. Beyond conventional immune-checkpoint inhibition - novel immunotherapies for renal cell carcinoma. Nature reviews Clinical oncology. 2021;18:199–214.
31. Şenbabaoğlu Y, Gejman RS, Winer AG, Liu M, Van Allen EM, de Velasco G, et al. Tumor immune microenvironment characterization in clear cell renal cell carcinoma identifies prognostic and immunotherapeutically relevant messenger RNA signatures. Genome biology. 2016;17:231.
32. Vuong L, Kotecha RR, Voss MH, Hakimi AA. Tumor Microenvironment Dynamics in Clear-Cell Renal Cell Carcinoma. Cancer discovery. 2019;9:1349–57.
33. Cannarile MA, Weisser M, Jacob W, Jegg A-M, Ries CH, Rüttinger D. Colony-stimulating factor 1 receptor (CSF1R) inhibitors in cancer therapy. Journal for immunotherapy of cancer. 2017;5:53.
34. Omland H, Fosså SD. Spontaneous regression of cerebral and pulmonary metastases in renal cell carcinoma. Scandinavian journal of urology and nephrology. 1989;23:159–60.
35. Tanaka M, Fukuda H, Higashi Y. [A case of complete regression of metastatic renal cell carcinoma following corticosteroid treatment]. Hinyokika kiyo Acta urologica Japonica. 2003;49:225–8.
36. Christophersen AO, Lie AK, Fosså SD. Unexpected 10 years complete remission after cortisone mono-therapy in metastatic renal cell carcinoma. Acta oncologica (Stockholm, Sweden). 2006;45:226–8.
37. Schöffski P, Wolter P, Vandenborre K, Haustermans K. Clinical response of renal cell carcinoma to dexamethasone. Cancer investigation. 2009;27:529–32.
38. Janiszewska AD, Poletajew S, Wasiutyński A. Spontaneous regression of renal cell carcinoma. Contemporary oncology (Poznan, Poland). 2013;17:123–7.
39. Huynh TP, Barwe SP, Lee SJ, McSpadden R, Franco OE, Hayward SW, et al. Glucocorticoids suppress renal cell carcinoma progression by enhancing Na,K-ATPase beta-1 subunit expression. PloS one. 2015;10:e0122442.
40. Arai Y, Nonomura N, Nakai Y, Nishimura K, Oka D, Shiba M, et al. The growth-inhibitory effects of dexamethasone on renal cell carcinoma in vivo and in vitro. Cancer investigation. 2008;26:35–40.
41. Lin K-T, Wang L-H. New dimension of glucocorticoids in cancer treatment. Steroids. 2016;111:84–8.
42. Iwai A, Fujii Y, Kawakami S, Takazawa R, Kageyama Y, Yoshida MA, et al. Down-regulation of vascular endothelial growth factor in renal cell carcinoma cells by glucocorticoids. Molecular and cellular endocrinology. 2004;226:11–7.
43. Climent N, Plana M. Immunomodulatory Activity of Tyrosine Kinase Inhibitors to Elicit Cytotoxicity Against Cancer and Viral Infection. Frontiers in pharmacology. 2019;10:1232.
44. Sun K-H, Sun G-H, Wu Y-C, Ko B-J, Hsu H-T, Wu S-T. TNF-α augments CXCR2 and CXCR3 to promote progression of renal cell carcinoma. Journal of cellular and molecular medicine. 2016;20:2020–8.
45. Harrison ML, Obermueller E, Maisey NR, Hoare S, Edmonds K, Li NF, et al. Tumor necrosis factor alpha as a new target for renal cell carcinoma: two sequential phase II trials of infliximab at standard

and high dose. Journal of clinical oncology : official journal of the American Society of Clinical Oncology. 2007;25:4542–9.

46. Ou Y-C, Yang C-R, Cheng C-L, Raung S-L, Hung Y-Y, Chen C-J. Indomethacin induces apoptosis in 786-O renal cell carcinoma cells by activating mitogen-activated protein kinases and AKT. European journal of pharmacology. 2007;563:49–60.
47. Gregorian SK, Battisto JR. Immunosuppression in murine renal cell carcinoma. II. Identification of responsible lymphoid cell phenotypes and examination of elimination of suppression. Cancer immunology, immunotherapy : CII. 1990;31:335–41.
48. DeNardo DG, Galkin A, Dupont J, Zhou L, Bendell J. GB1275, a first-in-class CD11b modulator: rationale for immunotherapeutic combinations in solid tumors. Journal for immunotherapy of cancer. 2021;9.
49. Hemmatazad H, Berger MD. CCR5 is a potential therapeutic target for cancer. Expert opinion on therapeutic targets. 2021;25:311–27.
50. Zeng Z, Lan T, Wei Y, Wei X. CCL5/CCR5 axis in human diseases and related treatments. Genes & diseases. 2022;9:12–27.
51. Zhou Q, Qi Y, Wang Z, Zeng H, Zhang H, Liu Z, et al. CCR5 blockade inflames antitumor immunity in BAP1-mutant clear cell renal cell carcinoma. Journal for immunotherapy of cancer. 2020;8.
52. Jiang YL. Design, synthesis and spectroscopic studies of resveratrol aliphatic acid ligands of human serum albumin. Bioorganic & medicinal chemistry. 2008;16:6406–14.
53. Tian X, Zhang S, Zhang Q, Kang L, Ma C, Feng L, et al. Resveratrol inhibits tumor progression by down-regulation of NLRP3 in renal cell carcinoma. The Journal of nutritional biochemistry. 2020;85:108489.
54. Dai L, Chen L, Wang W, Lin P. Resveratrol inhibits ACHN cells via regulation of histone acetylation. Pharmaceutical biology. 2020;58:231–8.
55. Chen L, Yang S, Liao W, Xiong Y. Modification of Antitumor Immunity and Tumor Microenvironment by Resveratrol in Mouse Renal Tumor Model. Cell biochemistry and biophysics. 2015;72:617–25.
56. Zeng Y, Li F, Shi C-W, Du J-L, Xue Y-J, Liu X-Y, et al. Mechanism and therapeutic prospect of resveratrol combined with TRAIL in the treatment of renal cell carcinoma. Cancer gene therapy. 2020;27:619–23.

Tables

Table 1

Top 10 enriched terms of gene ontology and Reactome pathway analysis for the DEGs in the disease highly correlated module.

Enrichment	Terms	% Associated Genes / Fold enrichment (GO terms)	Adj p-value
Reactome	Translocation of ZAP-70 to Immunological synapse (R-HSA:202430)	73.68	5.26E-07
	Endosomal/Vacuolar pathway (R-HSA:1236977)	72.72	0.003022695
	Interleukin-10 signaling (R-HSA:6783783)	44.68	1.58E-05
	Immunoregulatory interactions between a Lymphoid and a non-Lymphoid cell (R-HSA:198933)	44.36	6.80E-18
	Cell surface interactions at the vascular wall (R-HSA:202733)	29.71	2.28E-05
	Toll-like Receptor Cascades (R-HSA:168898)	27.67	5.76E-05
	Cytokine Signaling in Immune system (R-HSA:1280215)	25.97	4.16E-23
	Neutrophil degranulation (R-HSA:6798695)	23.75	3.22E-10
	Immune System (R-HSA:168256)	23.34	1.15E-53
	Class A/1 (Rhodopsin-like receptors) (R-HSA:373076)	20.89	0.002052843
BP	negative regulation of neutrophil activation (GO:1902564)	8.96	4.35E-02
	interleukin-2-mediated signaling pathway (GO:0038110)	8.96	4.34E-02
	Fc receptor mediated inhibitory signaling pathway (GO:0002774)	8.96	4.33E-02
	interleukin-27-mediated signaling pathway (GO:0070106)	7.68	2.61E-02
	interferon-gamma-mediated signaling pathway (GO:0060333)	6.72	2.98E-05
	antigen processing and presentation of endogenous peptide antigen via MHC class I via ER pathway, TAP-independent (GO:0002486)	6.72	4.00E-02
	regulation of CD8-positive, alpha-beta T cell proliferation (GO:2000564)	6.72	3.98E-02
	response to interleukin-15 (GO:0070672)	6.72	3.98E-02
	regulation of neutrophil degranulation	6.72	3.97E-02
	regulation of hypersensitivity (GO:0002883)	6.72	3.96E-02

MF	TAP binding (GO:0046977)	7.84	4.71E-02
	T cell receptor binding (GO:0042608)	7.17	3.10E-02
	MHC class I receptor activity (GO:0032393)	5.48	1.48E-02
	pattern recognition receptor activity (GO:0038187)	4.65	7.11E-03
	MHC class II protein complex binding (GO:0023026)	4.31	1.93E-02
	NAD+ nucleosidase activity (GO:0003953)	4.16	2.37E-02
	peptide antigen binding (GO:0042605)	3.98	8.01E-03
	cytokine receptor activity (GO:0004896)	3.79	6.11E-08
	tumor necrosis factor receptor binding (GO:0005164)	3.64	4.92E-02
	cytokine binding (GO:0019955)	3.03	5.62E-07
CC	complement component C1 complex (GO:0005602)	8.96	3.81E-02
	MHC class I protein complex (GO:0042612)	6.97	1.35E-02
	MHC class II protein complex (GO:0042613)	5.97	6.65E-04
	NLRP3 inflammasome complex (GO:0072559)	5.97	4.81E-02
	MHC class I peptide loading complex (GO:0042824)	5.97	4.77E-02
	integral component of lumenal side of endoplasmic reticulum membrane (GO:0071556)	4.94	1.95E-04
	phagocytic cup (GO:0001891)	3.84	1.05E-02
	immunological synapse (GO:0001772)	3.33	5.15E-03
	tertiary granule membrane (GO:0070821)	3.19	1.78E-04
	ER to Golgi transport vesicle membrane (GO:0012507)	2.94	3.73E-03

BP: Biological process; MF: Molecular function; CC: Cellular component

Table 2

Top identified DEGs in the protein-protein interaction network (based on degree) and in the disease most correlated module (based on kME and GS values). Common DEGs (12 hub genes) are bold and underlined.

Top 100 DEGs in the PPI network	Top DEGs in the pink module
LCK, CD4, ANXA5, CD8A, EGF, ITGB3, EZH2, BUB1B, **CSF1R**, MTOR, CDH1, HRAS, VWF, PLK1, ITGB1, BDNF, STAT1, CDC20, PCNA, **RAC2**, CD80, HIF1A, EGFR, **TYROBP**, IL10, GAPDH, CCNA2, PPARA, ITGAX, IL13, **TLR2**, CCNB1, KDR, ATM, CCND1, IL15, TOP2A, APOE, BRCA1, **PLEK**, KIT, RELA, MYC, IFNG, CTLA4, CASP3, ERBB2, CXCL12, **CCL5**, AURKA, ICAM1, FOXP3, IL1B, ASPM, **CD86**, CD34, **PTPRC**, TLR4, CHEK1, KIF23, MAPK14, CDK1, AURKB, NRAS, **ITGAM**, INS, CD40, LRRK2, CDC6, PECAM1, CD28, ALDH18A1, CAV1, CXCL10, JUN, CD274, SPI1, RAD51, FN1, CD44, TP53, PRKCA, HSP90AA1, KIF11, MMP9, CYCS, CAT, ALB, CDK2, VEGFA, **CCR5**, BUB1, MDM2, CXCR4, MAD2L1, NFKBIA, **LCP2**, SELL, **ITGB2**, CDKN2A	**TYROBP**, P2RX7, LAPTM5, IFI16, **ITGB2**, ENTPD1, LY86, FCER1G, TREM2, PSMB8, ISG20, C1QB, CTSS, **CD86**, CASP1, C1QA, MS4A7, C1orf162, PTPRE, NKG7, HLA-F, PSMB9, C1QC, TYMP, HCK, FPR3, APOC1, LINC01094, **ITGAM**, TAP1, HCLS1, LILRB2, IL10RA, ARHGDIB, C3AR1, DTX3L, CORO1A, IGSF6, BIRC3, ADORA3, MSR1, NMI, IL15RA, C3, SLC43A3, RGS1, CD300A, CRLF3, MS4A6A, FXYD5, **LCP2**, LST1, NINJ2, FCGR1B, CLEC4A, CD300LF, EVI2B, UBE2L6, RNASE6, TLR8, LAIR1, HLA-DMA, GBP2, TRIM22, SP110, CD14, TNFSF13B, THEMIS2, GGTA1P, CHST11, ADAP2, CD84, **PTPRC**, IL4I1, HLA-DPA1, NCKAP1L, SP100, EVI2A, NCF4, **TLR2**, IFNAR2, TIMP1, CLEC2B, FCGR2C, LYN, APBB1IP, **RAC2**, MNDA, CSTA, SLA, KLHL6, TNFRSF1B, PYCARD, CD247, PSMB10, VAV1, RCSD1, CXCL16, RHBDF2, PARVG, TLR7, MS4A4A, MYO1F, CSF2RA, GIMAP2, LILRB1, GPR65, DOCK2, NLRC5, HLA-DRA, ARHGAP9, OLFML2B, KLRD1 OAS2, WIPF1, SAMHD1, MICB, TNFAIP8L2, CD53, CSF2RB, SLC15A3, GZMA, HLA-DMB, **CCL5**, TBXAS1, HCST, IKZF1, AOAH, CLEC7A, RGS18, SLAMF8, NCF2, ARPC1B, NOD2, DOK3, ADA, MPEG1, GZMB, EHBP1L1, RHOG, TAGAP, FLJ32255, GZMH, LY96, TNFAIP3, **CSF1R**, MAN2B1, LCP1, **CCR5**, RASSF5, CD2, CST7, RGS19, SASH3, PTPN22, IL2RB, CCL4, BCL2A1, CYBB, TLR1, TRBC1, RUNX3, SAMSN1, ADAMDEC1, LOC101928429, **PLEK**, KIAA0930, PARP9, CRTAM, EOMES

Figures

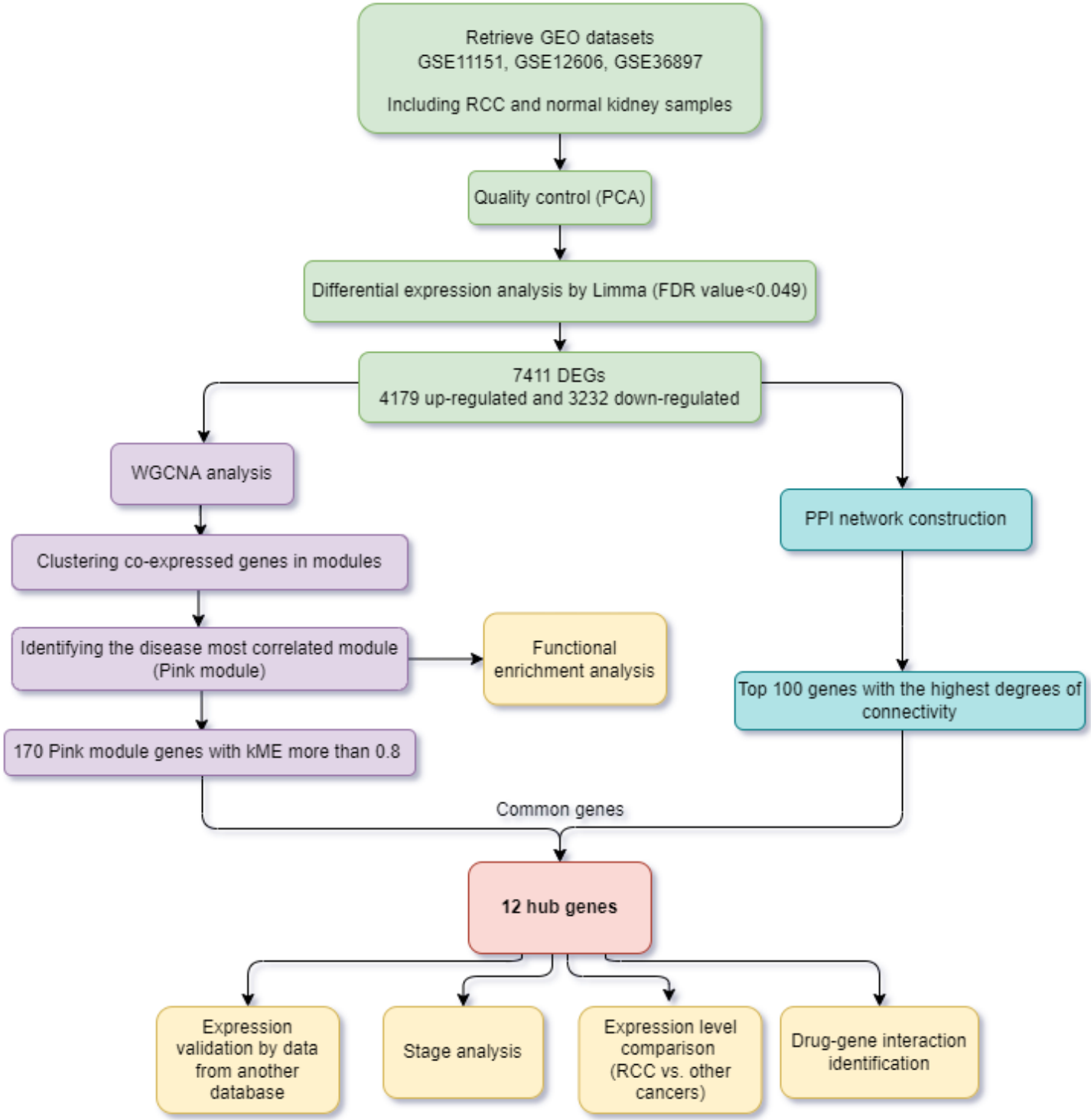

Figure 1

A flowchart representing the main steps of the present study. GEO, Gene Expression Omnibus; RCC, Renal cell carcinoma; PCA, principal component analysis; FDR, false discovery rate; DEGs, differentially expressed genes; WGCNA, weighted gene co-expression network analysis; PPI, protein-protein interaction; kME, module membership; GS, gene significance.

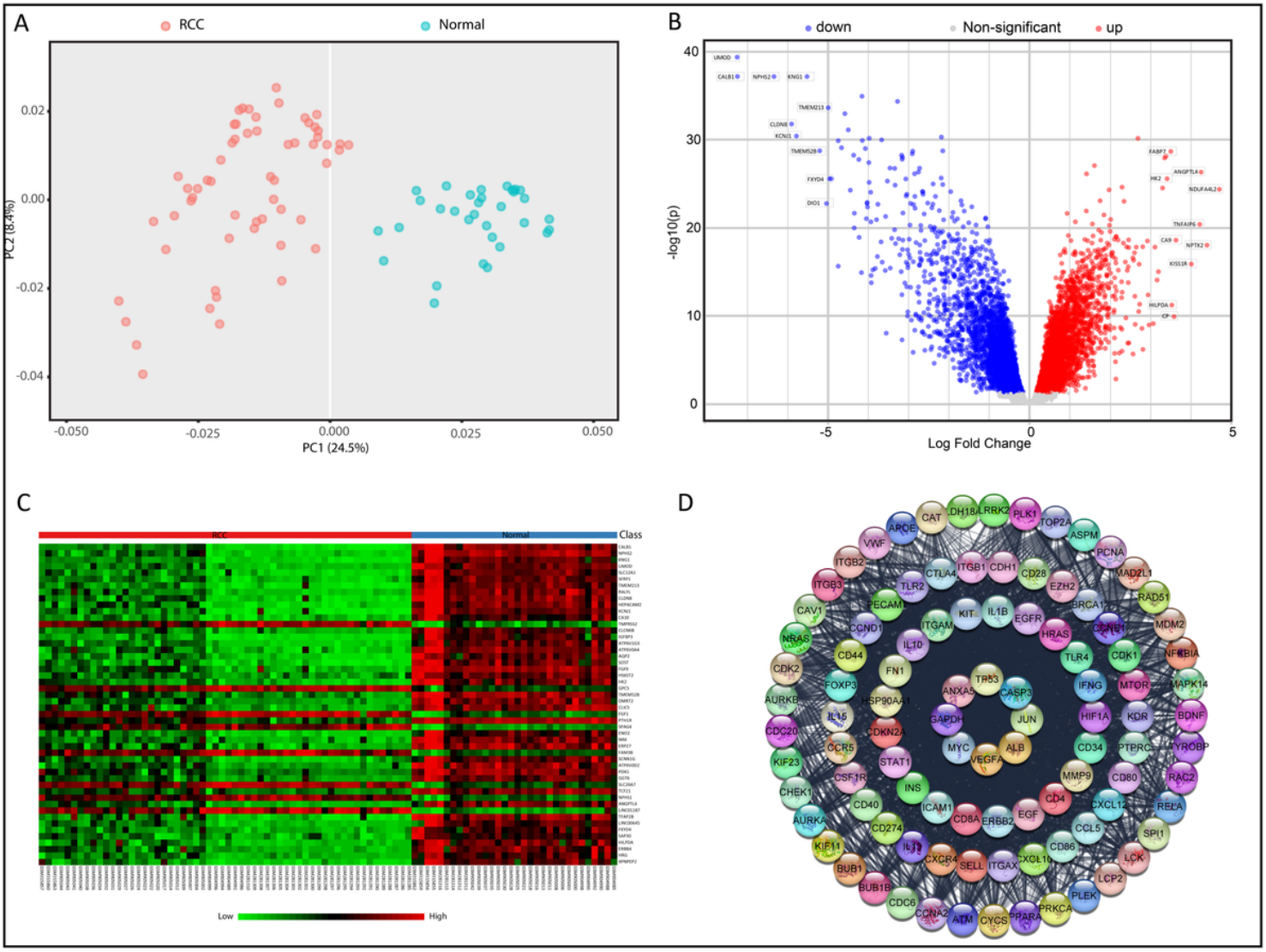

Figure 2

Data preprocessing and DEGs analysis; (A): PCA plot showing the similarities and differences among the RCC and normal samples; (B): Volcano plot of the analyzed dataset depicting top DEGs based on log2 fold change and adjusted p-value; (C): Heatmap of 50 top DEGs based of FDR value; (D). The top 100 genes (based on the degree of connectivity) in a PPI network, including all DEGs. The adjusted P-value < 0.05 was considered to select the significant DEGs.

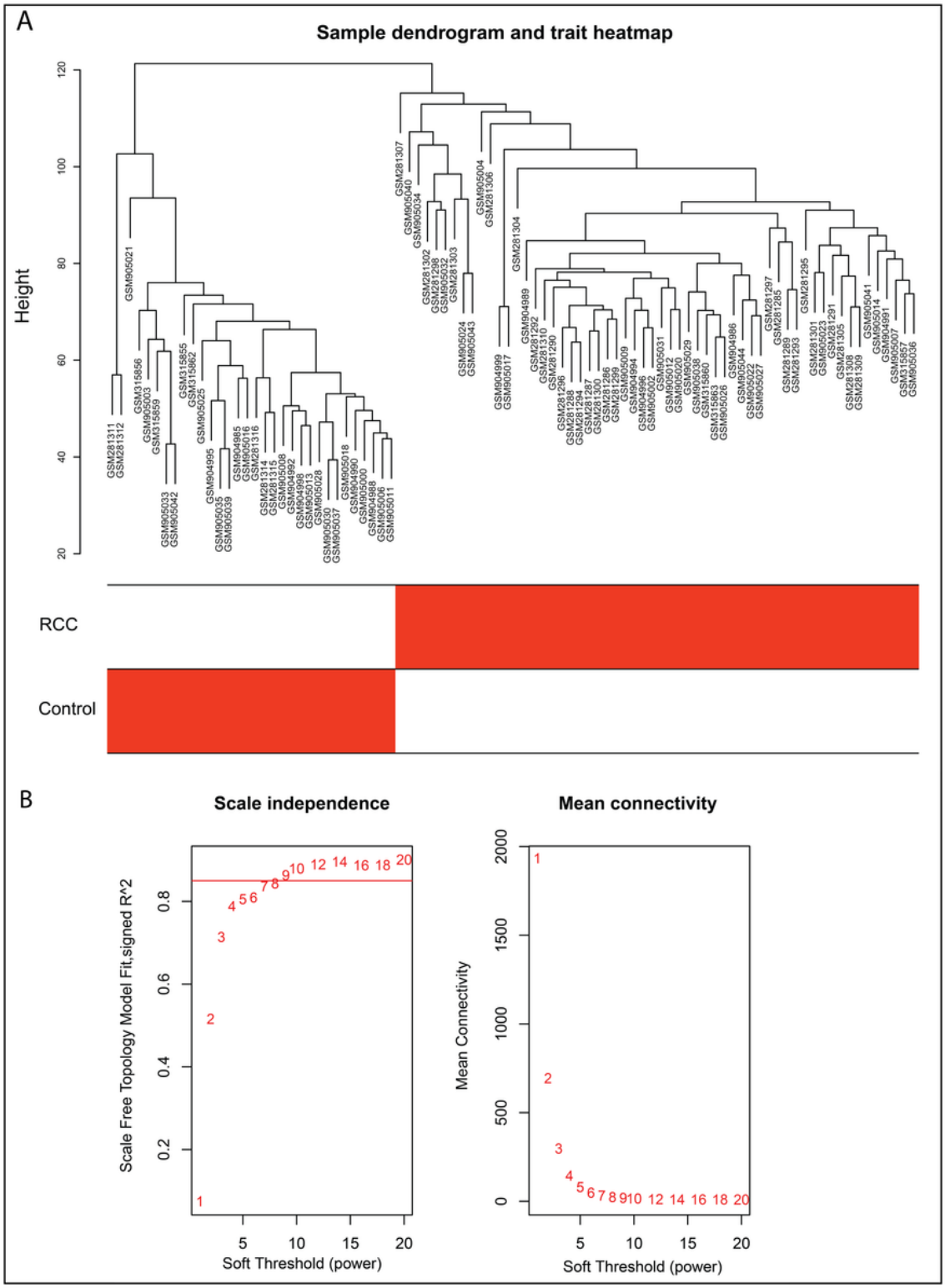

Figure 3

Sample clustering and approximation of the soft-thresholding value; (A): A dendrogram and trait heatmap representing the clustering of 58 RCC and 32 normal samples. (B). Two plots show the scale-free fit index and mean connectivity analysis results. Different values (1 to 20) were considered for the analysis. Based on the plots, the power of 7 was selected for the downstream analysis in the WGCNA algorithm.

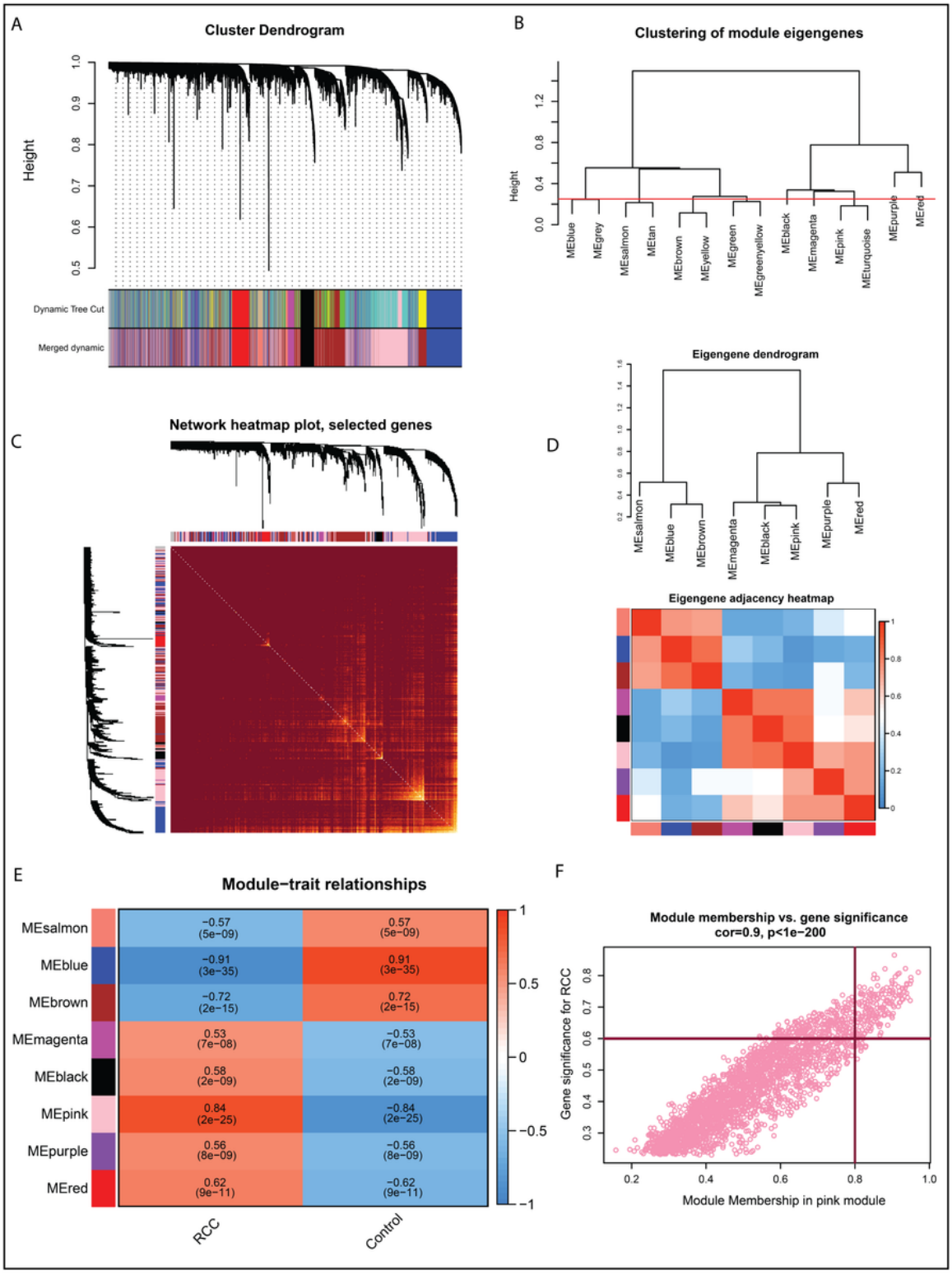

Figure 4

The results of WGCNA analysis; (A): Cluster dendrogram showing the clustered genes (branches) in co-expressed modules (different colors); (B): Clustering of module eigengenes and merging the modules (mergeCutHeight = 0.25); (C): Network heatmap plot of 1000 genes showing the module division

accuracy (each column and row belongs to a single gene; Progressive yellow color indicates higher adjacencies and red color indicates low adjacencies among genes in the modules); (D): Eigengene dendrogram and eigengene adjacency heatmap representing high (red) and low (blue) adjacencies among the modules; (E): The module-trait relationship plot showing the most positive correlated module to the clinical trait (RCC). (F). Scatter plot showing the gene significance (GS) and module membership (kME or MM) values of the clustered genes in the pink module; (Genes with kME $\geq$ 0.8 and GS $\geq$ 0.6 were considered as the hub).

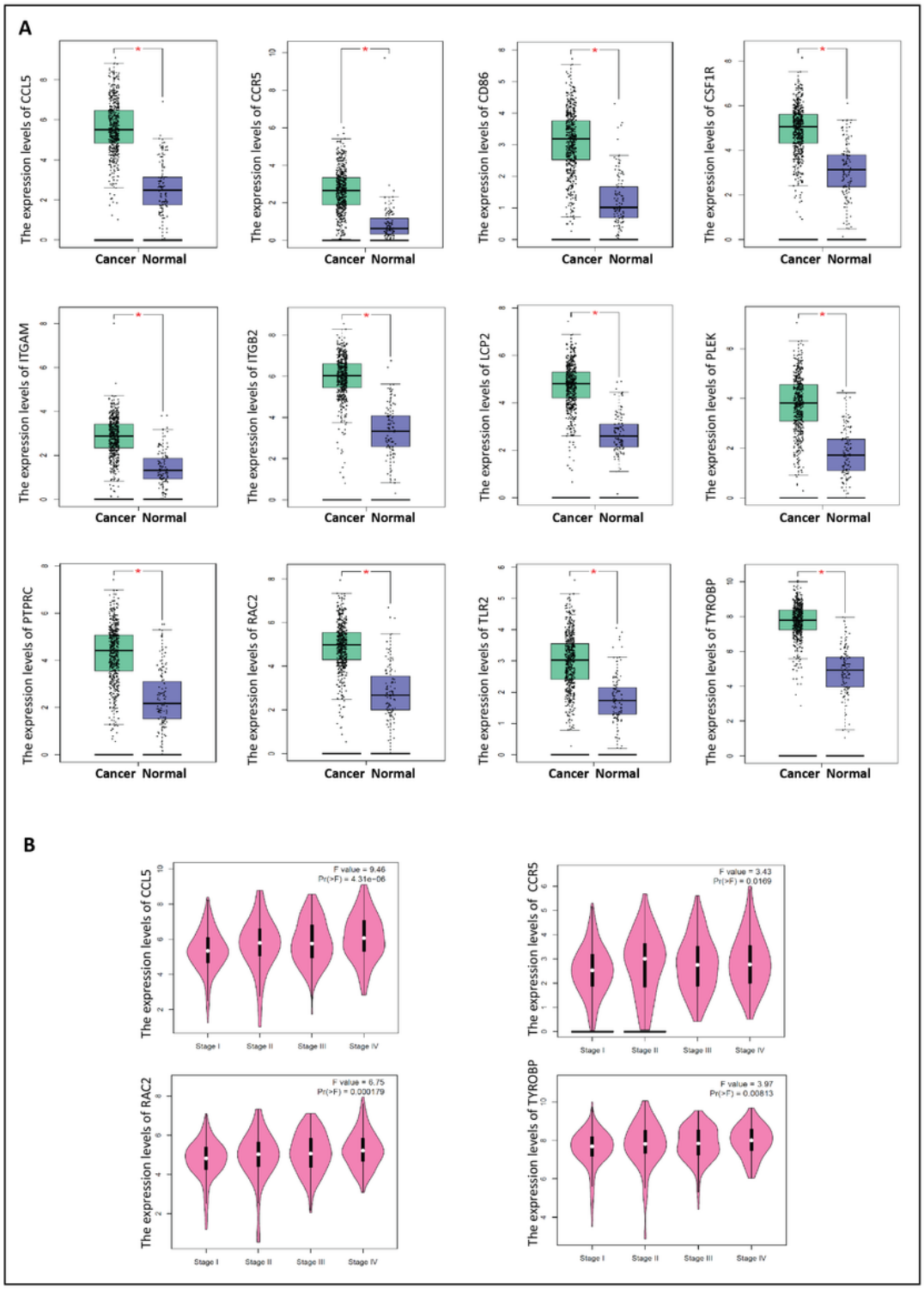

Figure 5

(A): GEPIA expression analysis of the ccRCC hub genes; (B): Pathological stage analysis of four hub genes.

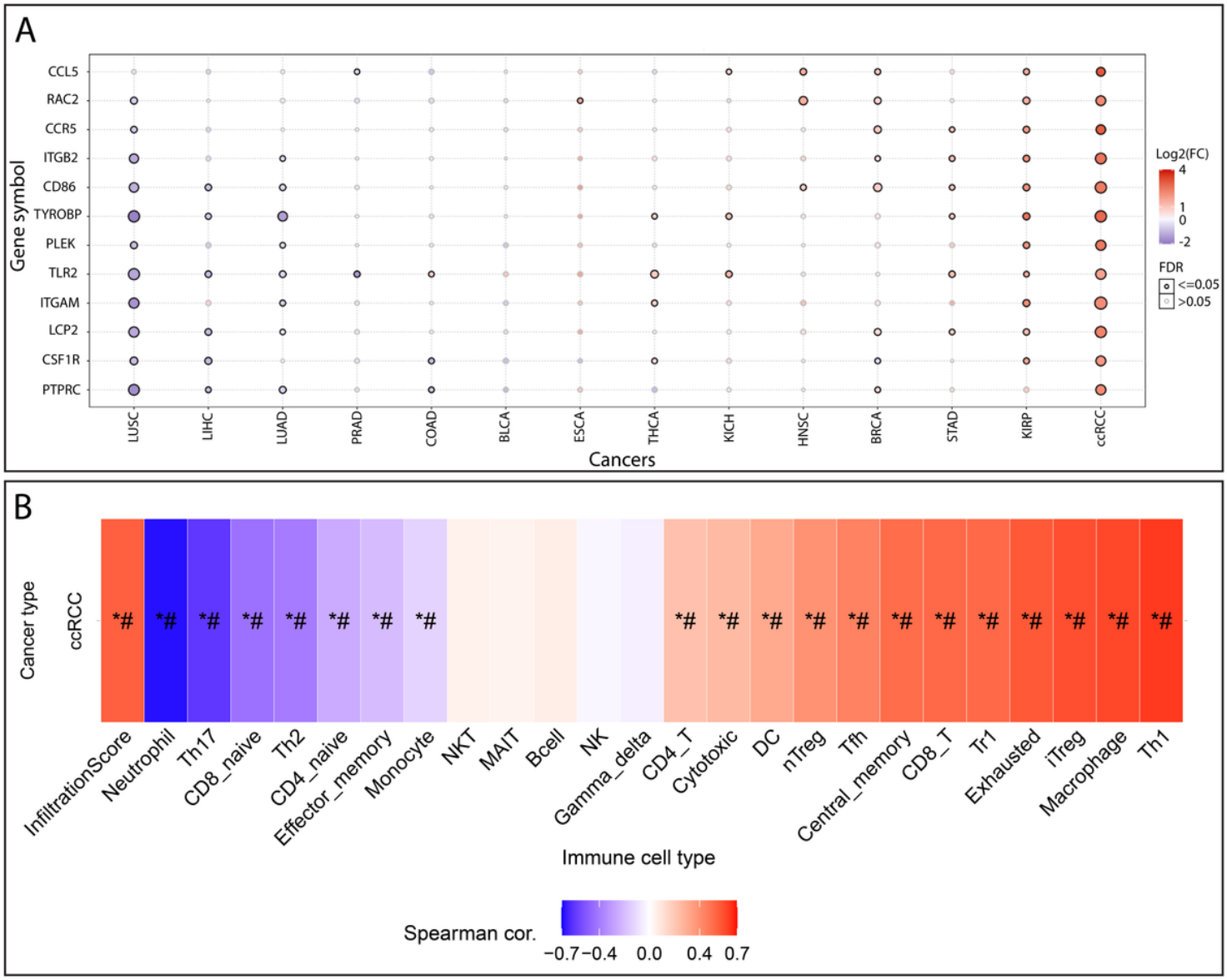

Figure 6

(A): The bubble plot of the fold changes of ccRCC hub genes compared to the other 13 cancer types by GSCA. These cancer types are THCA (Thyroid cancer), KIRP (Kidney renal papillary cell carcinoma), BLCA (Bladder Urothelial Carcinoma), LIHC (Liver hepatocellular carcinoma), HNSC (Head and neck squamous cell cancer), BRCA (Breast cancer), LUAD (Lung adenocarcinoma), PRAD (Prostate adenocarcinoma), ESCA (Esophageal carcinoma), KICH (Kidney chromophobe cancer), LUSC (lung squamous cell carcinoma), ccRCC (clear cell renal cell carcinoma), STAD (Stomach adenocarcinoma), and COAD (Colon adenocarcinoma). (B): The correlation between hub genes GSVA score and different immune cell infiltration. *: P-value ≤ 0.05; #: FDR ≤ 0.05.

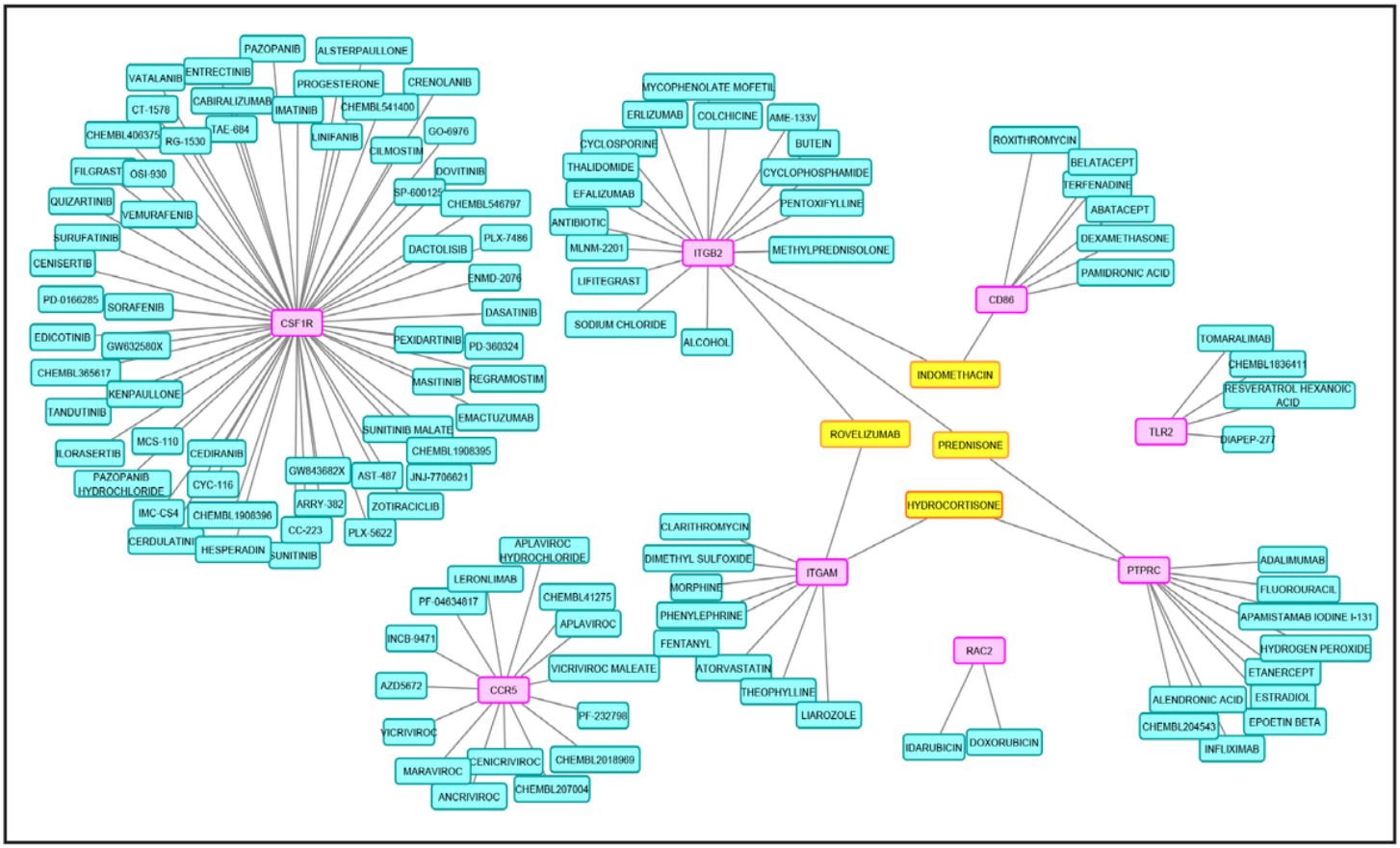

Figure 7

Network of potential drugs and targeted hub genes constructed by Cytoscape. The pink nodes are the targeted hub genes, and the turquoise nodes are potential drugs.

Supplementary Files

This is a list of supplementary files associated with this preprint. Click to download.

- Supplementaryfile1ListofDEGs.xlsx
- Supplementaryfile2Abriefdescriptionoftheidentifiedhubgenes..docx